Earth Surf. Dynam. Discuss., doi:10.5194/esurf-2016-55, 2016
Manuscript under review for journal Earth Surf. Dynam.
Published: 8 November 2016

Earth Surface Dynamics Discussions Open Access

Assessment of structural sediment connectivity within catchments: insights from graph theory

Étienne Cossart[1], Mathieu Fressard[1]

[1]Université de Lyon (Jean Moulin, Lyon 3), UMR 5600 CNRS – Environnement Ville Société, Lyon, 69007, France

Correspondence to: Étienne Cossart (etienne.cossart@univ-lyon3.fr)

Abstract. To understand the sedimentary signal delivered at catchment outlets, many authors now refer to the concept of connectivity. In this framework, the sedimentary signal is seen as an emergent organization of local filiations and interactions. The challenge is then to open black boxes that remain within a sediment cascade, that requires both accurate geomorphic investigations in the field (reconstruction of sequences of geomorphic evolution, description of sediment pathways) but also the development of tools dedicated to sediment cascades modelling. More precisely the development of tools dedicated to the study of connectivity in geomorphology is still in progress, even if the graph theory offers promising perspectives (Heckmann and Schwanghart, 2013). In this paper, graph theory is applied to abstract the network structure of sediment cascades, keeping only nodes (sediment sources, sediment stores, outlet) and links (linkage by a transportation agent), represented as vertices and edges. From the description of the assemblages of sedimentary flows, we provide three main indices to explore how small-scale processes may result in significant broad-scale geomorphic patterns. First, we assess the potential contribution of each node to the sediment delivery at the outlet. Second, we measure the influence of each node regarding how this node is accessible from both sediment sources and outlet. Third, we calculate a connectivity index to reveal whether the potential contribution of a node is lower or higher than expected from its location within the network. These indices are calculated in the case of a virtual sediment cascade, but are also applied to a catchment located in southern french alps. We demonstrate that these indices are robust, and may lead to simulations. In the present case, we try to predict how a sediment cascade may be impacted by a node disruption or by a reconnection.

1 Introduction

The concept of connectivity provides now an overarching framework in geosciences to better explore the functioning of catchments. Connectivity has been first defined in ecology to assess the spatial coherence of a system of landscape elements, a coherence that is necessary to maintain or restore ecological functions (Bennett, 2004). Following these pioneering discussions, it has been increasingly used by hydrologists to model hydrological connections patterns (Delahaye et al., 2001; Douvinet et al., 2008); Ali and Roy (2009) for instance summarize that hydrological connectivity can be seen as a function of available water volume (calculated from a hydrological balance) and the rate of transfer. More recently, connectivity has appeared as a fruiftul conceptual framework in geomorphology (Brierley et al., 2006; Wainwright et al., 2011; Fryirs, 2013):

Earth Surf. Dynam. Discuss., doi:10.5194/esurf-2016-55, 2016
Manuscript under review for journal Earth Surf. Dynam.
Published: 8 November 2016

it helps in studying the spatio-temporal unsteadiness of sediment transport within catchments, and why sediment cascades can be considered a "jerky conveyor belt" (Ferguson, 1981). Unsteadiness patterns in sediment transfers are indeed one main field of research for geomorphologists, and refer to the "spatial and temporal paradox" exhibited by McGuiness et al. (1971): in a catchment, sediment delivery from sources on hillslopes is not correlated with sediment delivery at the outlet. Consequently, sediment cascades are not necessarily efficient to transfer sediments, highlighting a "sediment delivery problem" (Walling, 1983). Finally, geomorphic signals, especially sediment delivery, cannot be interpreted easily (e.g. in terms of climate change, anthropogenic influences, etc.) and may much more reveal a "sedimentological anarchy" (Walker, 1990; Bravard, 1998; Schumm, 2005): at catchment scale geomorphic processes may be coupled to create of a sediment impulse, or may be antagonistic to create a blockage, alternately.

Recently, many authors asked for complex-systems approach to conceptualize the continuum of sediment transfer: how processes at local scales may be combined to understand the functioning of the whole sediment cascade (Fryirs et al., 2007; Borselli et al., 2008; Fryirs, 2013; Bracken et al., 2015). Such a multiscalar framework has been conceptualized by Heckmann and Schwanghart (2013) who have clearly distinguished the coupling of processes, and connectivity. On the one hand geomorphic coupling is "the linkage of distinct landforms or landscape units by sediment transport" (Harvey, 2001), it refers to "elementary interactions at the relatively small scale" (Faulkner, 2008). On the other hand "the degree of coupling, the combined effect of lateral (hillslope to channel) and longitudinal (from one river reach to another) linkages between system components, is termed (sediment) connectivity" (Heckmann and Schwanghart, 2013). Shifting from the local to the catchment scale remains a main issue to well explain how small-scale measurements of erosion result in broad-scale geomorphic patterns and processes (Bracken et al., 2015). It requires the development of numerical methods to draw exhaustive inventory of all the local linkages within the sediment cascades, to exhibit their properties, and then to predict the result of their combination. One promising field of research has been opened up by the application of graph theory, that offers mathematical tools to analyse statistically and spatially the assemblages of all the components of a sediment cascade (Heckmann and Schwanghart, 2013; Heckmann et al., 2015). This methodological framework particularly focuses on the structural connectivity, i.e. the influence of the spatial patterns drawn by the linkages on sediment delivery. One main objective is to provide a quantitative index that would help in comparing the geomorphic behaviour of catchments in both space and time. It would also allow an estimation of the contribution of a given part of the catchment to provide sediments at the outlet, and to interpret local erosion monitoring (Cavalli et al., 2013).

In this paper we seek at assessing such a connectivity index. Following a brief state-of-art regarding connectivity indices, we explore the main mathematical tools provided by graph theory to measure the structural sediment connectivity within a catchment. Then we look at the main applications and interpretations of connectivity index.

2 State-of-art

By stating that catchments are inefficient at supplying sediment to the outlet, Walling (1983) developed one pioneering study of catchments sediment connectivity. He exhibited that they are characterized by a low sediment delivery ratio (SDR).

SDR = Vh / Vo (1)

Where Vh is the volume of sediment eroded from hillslopes and Vo is the volume of sediment delivered at the outlet of the catchment. The SDR is a synthetic index that assesses the connectivity of a catchment, and allows comparisons in both space and time. Recently, it has for instance been demonstrated that SDR (and connectivity) decreases with increasing landscape morphological complexity (Baartman et al., 2013). One main criticism regarding this index is that catchments remain a black box: no attention is paid to the geomorphic linkages involved at local scale, nor to the feedbacks between geomorphic processes (Gumiere et al., 2011; Fryirs, 2013).

To open such black boxes, the concept of connectivity has been subdivided in two distinct parts (With et al., 1997; Tischendorf and Fahrig, 2000; Turnbull et al., 2008). On the one hand the structural connectivity refers to spatial patterns in the landscape, such as the spatial distribution of landscape units which influences sediment transfer patterns and sediment paths. On the other hand, the functional connectivity focuses on how geomorphic processes may activate or block the sediment transfer along the spatial links within the sediment cascade (Kimberly et al., 1997; With and King, 1997; Belisle, 2005; Uezu et al., 2005). The latter is now also often called process-based sediment connectivity and has been documented in depth in a recent review (Bracken et al., 2015). Here we focus on the structural connectivity, which quantification is required for exploring and understanding the responses of geomorphic systems (Wainwright et al., 2011).

2.1 Structural sediment connectivity

Following Borselli et al. (2008), Cavalli et al. (2013) developped a connectivity index (Eq. 2) that well refers to the structural connectivity. It estimates that connectivity at one location within the catchment can be seen as a ratio between an upslope (Eq. 3) and a downslope components (Eq. 4):

$$IC = \log_{10}\left(\frac{D_{up}}{D_{dn}}\right) \quad (2)$$

Dup = W S √A (3)

Ddn = ∑i di / Wi Si (4)

where W is the average weighting factor of the upslope contributing area, S is the average slope gradient of the upslope contributing area (m/m) and A is the upslope contributing area (m2) and where di is the length of the flow path along the ith cell according to the steepest downslope direction (m), Wi and Si are the weighting factor and the slope gradient of the ith cell, respectively. In Borselli et al. (2008) the weighting factor W first corresponded to the C-factor of USLE-RUSLE models (Wischmeier and Smith 1978; Renard et al. 1997) to refer to frictions that hinder the sediment transfer. More

Earth Surf. Dynam. Discuss., doi:10.5194/esurf-2016-55, 2016
Manuscript under review for journal Earth Surf. Dynam.
Published: 8 November 2016

recently, it has been demonstrated that topographic surface roughness can provide a good estimation of the weighting factor (Cavalli et al., 2013; Baartman et al., 2013): a great topographic heterogeneity impeding sediment transfer. This index opens up a fruitful field of research to assess the structural connectivity. First, it opens the black boxes within a catchment: the IC index can be calculated for each cell of the catchment, highlighted what are the cells that may highly contribute to the sediment flux at the outlet. Second, this index takes into account all the links that exist between a cell and all other components of the catchment: it nicely refers to the definition of connectivity. Third, the index can be mapped so that it allows comparisons between various locations (a specific tool has been developped in Arc GIS), and furthermore to calculate maps of connectivity evolution through time. Nevertheless, this index remains empiric, so that comparisons between catchments should be made carefully. More specifically, the units used during the calculation make the interpretation of the results complicated. Dup is indeed calculated in meters, Dds is calculated in meters-1, so that IC is expressed in m2.

Another promising field of research refers to the application of graph theory that provides a robust mathematical framework for describing networks such as sediment cascades (Heckmann and Schwanghart, 2013; Heckmann et al., 2015; Cossart, 2016). Graph theory is applied to abstract the network structure, keeping only nodes (sediment sources, sediment stores, outlet) and links (linkage by a transportation agent), represented as vertices and edges. The goal is to get a simple pattern that can be described by algebraic tools (typology of linkages, identification of local sinks, etc.) to exhibit the overall structure of the sedimentary cascade. Graph theory enables to describe objectively the assemblages of sedimentary flows, and thus to estimate the net contribution of the network to the amount of sediment load. Indices provided by graph theory were hitherto developed to characterize the properties of single landscape units (nodes), sediment pathways (edges) and sediment cascades (edge sequences = paths). The nodes can be characterized by the number and type of links that may provide or carry out sediments. Sediment sources are characterized by the lack of input link; sinks are characterized by no output link; and other nodes correspond to connector which importance is revealed by their degree (number of input and output links). The links may be characterized by the geomorphic process that carries sediments. Regarding the edge sequences their main characteristic is whether they may contribute or not the sediment delivery at the outlet: do they correspond to a connected component or not? The frequency and the preferential location of each type of nodes, edges and edge sequences are of prime importance to explain the SDR at the outlet (Heckmann and Schwanghart, 2013; Heckmann et al., 2015).

One another application is to conduct some "flow analyses": in a directed graph (such as sediment cascades) each edge has a capacity and each edge receives a flow. A flow must satisfy the restriction that the amount of flow into a node equals the amount of flow out of it, unless it is a source, which has only outgoing flow, or sink, which has only incoming flow. This is a simulation, to the extent that this analysis is based on an assumption of conservation of flow. In the case of sources having no incoming links, a default common value can be assigned to them. Sometimes called network effect (Pumain and Saint-Julien, 2010), it exhibits how the network structure predisposes and organizes sediment flows "all things being equal" (Cossart, 2016).

Earth Surf. Dynam. Discuss., doi:10.5194/esurf-2016-55, 2016
Manuscript under review for journal Earth Surf. Dynam.
Published: 8 November 2016

2.2 Structural connectivity indices in undirected graphs

The influence of the structure of a spatial network on a material or immaterial fluxes has been deeply explored in case of transportation studies (Cole and King, 1968; Gleyze, 2008), social networks (Freeman, 1979) or more recently in ecology (Ludwig et al., 2002; Belisle, 2005). In such studies, one key requirement is to provide a hierarchy of the influence of nodes within the network. Nodes characterized by a high connectivity have indeed a considerable influence within a network as they control fluxes passing between many others. Such high connectivity nodes are also the ones where a disruption would imply the more dramatic damages on the network functioning (Haggett and Chorley, 1969; Newman, 2010). They indeed lie on the largest number of possible paths whithin the network. Many indices were calculated from the mathematical tools provided by graph theory and applied to undirected graphs. Their signification may nevertheless help in understanding how the structural connectivity can be measured in directed graphs such as sediment cascades.

First, the Betweenness centrality index (B) measures the extent to which a node i lies on paths between other nodes (Eq. 5):

$$Bi = \sum nijk / njk \quad (5)$$

where nijk is the number of paths that exist from a node j to a node k, and that pass through i; and where njk is the total number of paths that exist within the network, from j to k. This index provides a good evaluation of the potential volume that may pass through the nodes and is helpful for interpreting, even normalizing the real fluxes observed in each node of the network. One main criticism is that this index enhances the role of nodes close the centre of gravity of the network and is not really efficient in discriminating the eccentric nodes. However, such eccentric nodes are close to the sources, the entrances, of the network and should be discriminated between themselves. Furthermore, spatial patterns are taken into account in a simplistic way: the distance (and the friction effect of the distance to hinder fluxes) is not considered.

The Shimbel index (Shi) takes into account the distance between nodes and consider whether the location of the node generates or minimize eccentricity within the network (Eq. 6) (Newman, 2010). For one node i, it corresponds to the sum of the length of all shortest paths connecting all other nodes j in the graph (dij). To facilitate comparisons in both space and time, this index should be normalized, being divided by the sum of the length of all paths in the network, from j to k (djk).

$$Shii = \sum dij / \sum djk \quad (6)$$

On the one hand if the Shimbel index is high, then the node contributes to create long paths within the network (and thus attenuates the compactness of the network). On the other hand, if the Shimbel index is low, then the node maximizes the compactness of the network. This index is much more efficient to discriminate the influence of eccentric nodes on the network and can be enriched by considering various types of distance (geodesic, time, etc.). It is noted that the lower the Shimbel index, the higher the accessibility (and thus the connectivity) of the nodes.

Both indices allow a description in depth of the skeleton of a network, and highlight the potential impacts of network structure on the fluxes patterns. They can thus provide conceptual and mathematical frameworks to explore the structure of sediment cascade. Nevertheless they cannot be applied directly to measure sediment connectivity as sediment cascades are directed graphs, more complicated in terms of mathematical conceptualization.

3 Methods to assess structural connectivity

Sediment cascades can be described as systems and network (Chorley and Kennedy, 1971; Schumm, 2005). In details, they may be represented by directed graphs, where the nodes correspond to landscape units (sediment sources, stores or sink) and the edges to sediment pathways (Heckmann et al., 2015). Two nodes i and j are joined or adjacent if there is an edge from i to j. Suppose we are given a directed graph with n nodes, the graph can be represented by an n × n adjacency matrix A, constructed as follows: if there is an edge from node i to node j, then we put 1 as the entry on row i, column j of the matrix A. In this study we first consider a virtual sediment cascade, with 7 nodes (Fig. 1).

3.1 Potential flows in directed graphs

As in undirected graphs, one first issue is to quantify the "network effect" (sensu Pumain and Saint-Julien, 2010) to enhance how the spatial structure of paths influences the amount of sediments transferred to the outlet. In sediment cascades, only the paths that come from one node j to the outlet o are to be considered, so that in each node i we have to measure the extent to which i lies on paths from other nodes j to o (Fijo). This measurement is normalized, thus subdivided by the total number of paths that come from all nodes j to o (Fjo) (Eq. 7).

$Fi = \sum Fijo / Fjo$ (7)

Fijo and Fjo can be calculated by reconstructing the pathways of sediments throughout the cascade. Under the hypothesis of "all things being equal", a virtual volume of sediments 1 is set on each node. The evacuation of the sediments can be simulated by a matrix multiplication of the adjacency matrix with a matrix representing the sediment sources (S0) (Eq. 8). This matrix is a one column matrix, where each row represents a node of the cascade, 1 is put on each row to represent the virtual volume of sediments at the beginning of the transfer. Each multiplication corresponds to an iteration, in which each sediment is transferred along one edge, according to the links described by the adjacency matrix (Eq. 9) (table 1). The result provides a matrix S1, highlighting where are the sediments after one single iteration.

$S1 = S0 \times A$ (8)

$Sn = Sn\text{-}1 \times A$ (9)

The operation is repeated until all virtual sediments are evacuated, and the results can represented within a synthetic matrix (S.), concatenating S0, S1,…, Sn matrices obtained during the calculation (table 2). This operation finally provides a first map of the potential flows within the sediment cascade. Such a result can be useful for interpreting local monitoring of sediment transfer, and then for interpolating local measurements at the catchment scale. Moreover, this index may provide a hierarchy between the nodes by assessing the increase of sediments involved upstream and upstream the node. For instance, in our virtual study case, the amount of sediment classically increases downstream, as there is no interruption of the cascade. Nevertheless, the main increase occurs apart node D, pointing out that this node has a great influence on the functioning of the sediment cascade. Any disruption of this node (blockage due to an overflow of sediments, anthropogenic action, etc.) would significantly impact the ability of the cascade to deliver sediments at the outlet. Nevertheless, on main criticism is that this index pay little attention to the sediment sources (here A, B and G) while the events that happen on it may influence long pathways to the outlet. As evoked for betweenness index, it is necessary to better discriminate the potential influence of sources and stores located next to sources.

3.2 Accessibility from sources and to sinks

Within a sediment cascade, the influence of geomorphic units (sources, stores, sinks) on sediment delivery can be discriminating by considering their location inside the cascades. The main hypothesis is that a node minimizing the distance between both sediment sources and the outlet has a greater influence on the overall sediment cascade. In other words, if such strategic nodes disrupt, the ability of the cascade to deliver sediment would be significantly affected. Characterizing the nodes by their location within the network refers to the concept of accessibility (A) and is thus very similar to the calculation Shimbel index in case of undirected graphs. In case of directed graphs, the calculation of the accessibility A of each node i can be made from a distance matrix D (Eq. 10) (table 3):

$$A_i = (D_{.i} + D_{i.}) / D_{..} \quad (10)$$

Where $D_{.i}$ is the total of the distances between I and the nodes (sources and stores) that feed i, $D_{i.}$ is the distance between i and the nodes located downstream, and $D_{..}$ is the total of the distances of all paths within the network. The main interest of this index is that it enhances the sources (where $D_{.i}$ equals 0), and more particularly the sources that minimize the distance to the outlet (Fig. 2). Here, G is characterized by the better accessibility, greater than A, greater than B. A hierarchy of the influence of sediment sources to sediment delivery at the outlet is thus provided. In terms of management, it highlights the sources that can be activated to cope with a sediment exhaustion at the outlet or, conversely, sources where protection strategies should be applied in case of sediment overflow. Nevertheless, this index is not a good proxy of connectivity as it underestimates the role of the outlet and all nodes close to the outlet, and does not pay attention to the coupling between various pathways inside the sediment cascade. At the catchment scale, the role of D and E is not exhibited while they are important connectors between pathways developed from sources A and B. It is necessary to compare carefully the index of both nodes to note that D minimizes more the distance to different sources and the outlet than E.

3.3 Combination of indices

The indices F_i and A_i provide a quantitative and complementary description of the sediment cascade skeleton, the first one revealing the potential increase of sediment discharge along the sediment paths, the second one measuring the eccentricity from the sources and the outlet. Classically, the sediment discharge increases with eccentricity from sources, as the paths lie across many nodes from which sediments can be supplied (i.e. the active area is higher). Nevertheless, due to the geometry of paths, of confluences, this increase of sediment discharge can be higher or lower than expected from the distance to sources. To estimate this possible under or overrepresentation of potential sediment volume in each node, a ratio between F_i and A_i can be calculated (Eq. 11):

$$IC_i = F_i / A_i \quad (11)$$

The results can be seen as a normalization of the potential sediment fluxes Fi (table 4). It is noticed that the most important nodes regarding IC are E and D (Fig. 3), with very similar values (0.8 and 0.71 respectively). E and D are at confluences and thus lie on various sediment paths organized from distinct sources: their potential influence on the whole sediment cascade is high, so that any disruption of these nodes would considerably alter the elementary interactions between many nodes and sediment paths. Consequently D and E may modify significantly the ability of the cascade to provide sediments and should be further studied in depth to document the functional connectivity, or to assess erosional rates (local monitoring, field observations). The outlet F has a quite high but lower index (0.66). This value reveals the high potential sediment volume that passes through this node but point out that any disruption at this node would be ambiguous. Indeed it would interrupt the sediment delivery, but the organization of the three sediment paths from sources A, B and G would be not modified, and the coupling patterns at the confluences would also remain unmodified. Finally, the structure of the cascade would be roughly unchanged. Regarding the sources (A, B and D): a hierarchy is evidenced. The source G has a greater influence on the sedimentary signal at the outlet thanks to its proximity (IC = 0.53), higher than A and B (IC equals to 0.27 and 0.12, respectively).

3.4 Index parameters

IC index can be calculated from simple parameters: adjacency matrix (drawn from a geomorphic expertise), distance matrix. Nevertheless two main components of the equations can be parameterized to enrich the model, for instance to fit the index to the geomorphic purpose or to a management issue. First, regarding the assessment of Fi, all sources are assumed to be of equal importance (volume availability equals to 1). A geomorphic hierarchy of sources (in terms of sediment supply) can be parameterized, for instance if a source particularly overflows or, conversely, is exhausted: the matrix representing the sediment sources (S0) can then be adjusted. Second, the distance is an important parameter that can modify the results of Ai, and then ICi. Distance indeed creates a friction that hampers the sediment transfer: the higher the distance, the higher the friction opposed to sediment delivery. In the virtual study case, we considered a topological distance within the matrix to be simple. Many other kinds of distance can of course be taken into account: Euclidian distance for instance, but in geomorphology many other type of distance may be more relevant. A distance in time, to reveal the duration of transfer from one unit to another one can be particularly relevant, even difficult to assess. A cost distance should be also relevant, by revealing how hampered (or efficient) is the sediment transfer along the edge: a manning coefficient (Cavalli et al., 2013), or more generally a roughness index (Baartmann et al., 2013) can be a good proxy of the friction that hampers the sediment transfer. Such parameters can be calculated from high-resolution DEM and then joined to the edges characteristics through GIS procedures.

To document how the indices are sensitive to the parameterization, we modify the initial conditions of our virtual sediment cascade (Fig. 4). Regarding sediment availability, we consider G exhausted (volume equals 0) and B overflowing (volume equals 2). All other nodes remain unchanged. Regarding the distance, the distance between E and F is now twice the initial value (DEF equals 2).

As expected, the potential flow Fi is mainly modified on B which influence increases (FB shifting from 0.05 to 0.07), and on G which influence becomes null. On other nodes, a significant increase is observed on D (FD shifting from 0.18 to 0.21) while FE and FF remain roughly unchanged. While the node D was already strategic in the first simulation, the increase of sediment availability on B reinforces its influence on the whole sediment cascade. Downstream, the potential flow on E and F is not reinforced by the amount of sediments delivered on B because of the exhaustion of G.

Considering the accessibility, the higher eccentricity of F has an impact on AF, but more generally alter the accessibility of all nodes. Accessibility decreases significantly on B: the subcascade organized from B is the longest and all the sediment paths that may exist along this subcascade are impacted by the friction between E and F. As a consequence, the outlet is here significantly less accessible from the source B than from the sources A and G (the latter remaining the closer). It is noticed that the accessibility of D is not impacted by the higher eccentricity of F: AD remains roughly stable, and even suggest a slight improvement of the accessibility. All nodes characterized by a great centrality, and that may minimize the distances from both the sources and the outlet, are not affected by an increasing eccentricity at the margins of the cascade (if distance from sources, or at the outlet, increases).

Finally, regarding the connectivity index, the new parameterization have modified the hierarchy of nodes. First we note that the influence of the confluence nodes has increased: this pattern is particularly significant on D, a node of a high connectivity: it minimizes the distance to two main sources and to the outlet. The node E is also of prime importance, but its connectivity is quite lower than expected from its strategic location as it is connected to an exhausted source (G). Looking at the sources, a hierarchy is clearly observed: the influence of B gets higher due to its main contribution to the sediment flow, while the influence of G becomes null as it is exhausted.

The IC index thus reveals on each unit of a sediment cascade the degree of coupling to both the sources and the outlet. More precisely it reflects the structural connectivity as it enhances the role of spatial patterns (distance, confluences, etc.) of the network. In a simplistic way, it highlights how the network structure and the spatial patterns influence the sediment flows "all things being equal". The parameterization could moreover be progressively enriched thanks to a geomorphic expertise to pay more attention on sediment availability or on the ability of geomorphic processes to transfer sediments along the paths (i.e. the edges).

4 Applications to real sediment cascade

The IC index is now applied to a real sediment cascade, which functioning has been already conceptualized and quantified (Cossart and Fort, 2008; Cossart, 2016). Celse-Nière catchment is located in the french southern Alps, on the eastern flank of the massif des Ecrins. We focus here on the headwater (about 10 km², from 2500 m.asl to 3850 m.asl), still occupied by glaciers. Special attention was already given to the linkages between the glacial margins and the glacio-fluvial systems. The presence of morainic ridges still interrupts the sedimentary cascade system, thus forcing local aggradation and change in the glacio-fluvial pattern (Fig. 5A). Such a complex assemblage makes this area particularly suitable for assessing connectivity and simulate the impacts of new blockages or, conversely, of some reconnections.

4.1 The structure of the network

From the geomorphological map, the graph has been drawn in a GIS software (QGIS): a regular network of nodes has been created (distance between nodes equals 100 meters). Each node is first characterized by the geomorphic unit to which it belongs, and from geomorphic expertise the linkages between the nodes are digitized. From the network QGIS tools, the adjacency matrix has been set (as an edge list matrix) and exported to R software. In the latter software, the matrix has been converted to an origin-to-destination matrix, and the distance matrix automatically created (a topological distance has been considered) thanks to the igraph package. All calculations on matrices have been conducted in R, and the results have been exported to QGIS to be mapped.

First it can be noticed that only 60% of the total paths are connected to the outlet, the others are connected to permanent sinks. By applying the typology established by Fryirs et al. (2007), disconnections are due to barriers (morainic ridges), buffers (roches-moutonnées and glacio-fluvial terraces) and blankets (screes made of large grain-size boulders) (Fig. 5B). Second, the IC index highlights the influence of the trunk valley located between the margin of Glacier-du-Sélé and the confluence with the Coup-de-Sabre proglacial river (Fig.6A). This observation can be interpreted in terms of sensitivity to external factors at the catchment scale. On the one hand, high-connectivity nodes (e.g. along the trunk valley, the Coup-de-Sabre subcatchment) are able to transfer along the cascade a perturbation due to a geomorphic event. A significant input of sediments (due for instance to hydro-meteorological event) in these areas would increase the sediment delivery at the outlet. On the other hand, any perturbations on the non-connected nodes (e.g. on the southern flank of Ailefroide) would have a null influence on the sediment delivery. The IC index also exhibits a hierarchy between the sources. As they are significantly closer to the outlet all the sources located in the Coup-de-Sabre subcathment have a greater influence on sediment delivery than the sources located in the Ailefroide, Sélé or Boeufs-Rouges areas.

Thus, the map of IC index helps to conceptualize the continuum of sediment transfer, and helps in interpreting monitoring measurements at one point in a catchment (not necessarily at the outlet). The examination of nodes connectivity may be required to establish sampling strategies for small-scale measurements of erosion on the field. Furthermore, this first examination highlights that the impacts of external drivers (anthropogenic impact, hydro-meteorological event and more generally climate change) are space dependent: the impacts are higher and efficiently propagated if they affect high-connectivity areas.

4.2 What if…?

The connectivity hierarchy between nodes can be interpreted as the potential influence of the node on sediment delivery, on the global functioning of the cascade. The IC index and more generally tools provided by graph theory allows simulation to predict what can be the more impacting events on the cascade. Two algorithms were here applied in R to simulate the consequences a local disconnection and a local reconnection.

First it has been asked to remove a node to create the more significant drop in terms of connectivity (Fig. 6B). This simulation can reflect the possible impact of an anthropogenic feature (e.g. a dam) or of a hillslope process (e.g. a dam created by a landslide mass or a debris flow). The greater impact would occur if the node located at the toe of Glacier du Sélé disrupts. It would imply the disconnection from the outlet of three main subcascades (organized from Ailefroide, Sélé and Boeufs-Rouges sources) so that only 26% percent of the nodes would remain connected to the outlet. The disruption would be more significant than in the case of a disruption of the node located at the confluence with Coup-de-Sabre proglacial river. In this latter case, many nodes would be indeed disconnected from the outlet, but the three subcascades of Ailefroide, Sélé and Boeufs-Rouges would be less impacted and would be still self-organized. As a consequence, the structure of the sediment cascade would be less modified.

Second, it has been queried to add a new linkage to create the better improvement of the overall sediment connectivity (Fig. 6C). This simulation can reflect the disruption of a barrier, the removal of a blanket, for instance following a high magnitude geomorphic event. In that case, a link between Guyard subcatchment and the trunk valley would create the highest IC value at the confluence. Such an increase is due to the high number of nodes that would become connected to the outlet. Furthermore these nodes (especially the sources) are relatively close to the outlet. A reconnection of subcascade in Ailefroide area would have a lesser impact because of its eccentricity. It can be noticed that the reconnection of Guyard subcascade would decrease the influence of Coup-de-Sabre subcascade on the overall network: under this hypothesis of reconnection, all the sources of this area are affected by a decrease of IC index. According to this new structure of the cascade, the hierarchy of sources would be thus modified: the sources of Guyard area would have a greater influence than Coup-de-Sabre sources, which would have a greater influence than Ailefroide, Sélé and Boeufs-Rouges sources.

As a consequence, the IC index provides an exploration of the cascade structure and may explain to what extent a small-scale modification (disruption of a node, creation of a linkage) may result in significant broad-scale geomorphic patterns and processes. More generally, IC index makes possible comparisons. In this study case comparisons have be made between cascades of different sizes, suggesting that IC index is sufficiently robust to allow comparisons in both space and time between various catchments.

5 Conclusion

This paper seeks at developing an original methodology dedicated to the study of sedimentary cascades under the hypothesis that connectors and paths influence on sediment delivery is space-dependent. The methods rely on graph theory to assess structural connectivity: sediment cascade is described as a network and consequently as graph. Inspired from indices developed in undirected graphs, a potential flow and an accessibility of geomorphic units (i.e. accessibility to both sediment sources and to the outlet) can be measured throughout the sediment cascade. Both indices are combined to estimate a connectivity index that reveals how influent is a node within a sediment cascade. Specific applications were led in a GIS software (QGIS) but also in software dedicated to data analysis and matrices calculations (R).

The application on a virtual and simple catchment, and then on a real catchment, exhibits how geomorphic processes filiations may lead (or not) to sediment mobilization and exportation, from upper slopes to the outlet of watersheds. The behaviour of the sediment cascades appears space-dependent: the geometry of paths and the location of nodes have a direct influence on the structural connectivity and then on the ability of the sediment cascade to deliver sediments. It is also highlighted that the impact of an external force on the sediment cascade depends on the location where it acts: the higher the connectivity of the node, the higher the impact on the cascade. Some simulations can moreover be led to predict how local perturbations may have an impact on the overall cascade.

This issue relies on main challenges in geomorphology and may lead to deep applications on river management, especially in Western Europe where rivers are affected by a strong deficit of sediment load. An assessment of connectivity will help at describing coupling patterns, scale dependence of erosional processes, to understand and predict how policies at catchment scale may supply sediments to the river system (dismantlement of hydraulic infrastructures, changes in terms of land use, etc.).

References

Ali, G.V. and Roy, A.G.: Revisiting hydrologic sampling strategies for an accurate assessment of hydrologic connectivity in humid temperate systems. Geography Compass 3, 350–374, 2009

Baartman, J.E.M., Masselink, R., Keesstra, S.D. and Temme, A.J.A.M. : Linking landscape morphological complexity and sediment connectivity. Earth Surface Processes and Landforms 38, 1457–1471, 2013.

Belisle, M.: Measuring landscape connectivity: the challenge of behavioural landscape ecology. Ecology 86, 1988–1995, 2005.

Bennett, G. : Integrating biodiversity conservation and sustainable use. Lessons learned from ecological networks. World Conservation Union (IUCN), Gland, Switzerland, 2004.

Brierley, G., Fryirs, K. and Jain, V. : Landscape connectivity: the geographic basis of geomorphic applications. Area 38(2), 165–174, 2006.

Borselli, L., Cassi, P. and Torri, D.: Prolegomena to sediment and flow connectivity in the landscape: a GIS and field numerical assessment. Catena 75, 268-277, 2008.

Bracken, L.J., Turnbull, J., Wainwright, J. and Bogaart, P.: Sediment connectivity: a framework for understanding sediment transfer at multiple scales. Earth Surface Processes and Landforms 40(2), 177-188, 2015.

Bravard, J.P.: Le temps et l'espace dans les systèmes fluviaux, deux dimensions spécifiques de l'approche géomorphologique. Annales de Géographie 107(599), 3-15, 1998.

Cavalli, M., Trevisani, S., Comiti, F. and Marchi, L.: Geomorphometric assessment of spatial sediment connectivity in small Alpine catchments. Geomorphology 188, 31-41, 2013.

Chorley, R.J. and Kennedy, B.A. Physical Geography: A Systems Approach. Prentice-Hall International, London, 370 pp, 1971.

Cole, J.P. and, King C.A.M. : Quantitative Geography: Techniques and theories in geography, Wiley, New York, 471 pp, 1968.

Cossart, É: La recrudescence de l'activité torrentielle dans un bassin versant en cours de déglaciation au cours du XXe siècle. Géomorphologie : relief, processus, environnement 3, 225-240, 2004.

Cossart, É. and Fort, M.: Sediment release and storage in early deglaciated areas: Towards an application of the exhaustion model from the case of Massif des Écrins French Alps since the Little Ice Age. Norsk Geografisk Tidsskrift – Norwegian Journal of Geography 62, 115-131, 2008.

Cossart, É.: L'(in)efficacité géomorphologique des cascades sédimentaires en question : les apports d'une analyse réseau. Cybergeo : European Journal of Geography 778, DOI : 10.4000/cybergeo.27625, 2016.

Delahaye, D., Guermond, Y. and Langlois, P.. Spatial interaction in the run-off process. Cybergeo : European Journal of Geography 213, DOI : 10.4000/cybergeo.3795, 2001.

Douvinet, J., Delahaye, D. and Langlois, P. : Modélisation de la dynamique potentielle d'un bassin versant et mesure de son efficacité structurelle. Cybergeo: European Journal of Geography 412, DOI : 10.4000/cybergeo.16103, 2008.

Faulkner, H.: Connectivity as a crucial determinant of badland geomorphology and evolution. Geomorphology 100(1-2), 91-103, 2008.

Ferguson, R.I.: Channel forms and channel changes. In: Lewin, J. (Ed.) British Rivers. Allen and Unwin, London. pp. 90-125, 1981.

Freeman, L.C.: Centrality in social networks conceptual clarification. Social networks 1(3), 215–239, 1979.

Fryirs, K.: DisConnectivity in catchment sediment cascades: a fresh look at the sediment delivery problem. Earth Surface Processes and Landforms Landforms 38, 30–46, 2013.

Fryirs, K., Brierley, G.J., Preston, N.J. and Kasai, M.. The disconnectivity of catchment-scale sediment cascades. Catena, 70, 49-67, 2007.

Gleyze, J.F.. Effets spatiaux et effets réseau dans l'évaluation d'indicateurs sur les nœuds d'un réseau d'infrastructure. Cybergeo: European Journal of Geography 370, DOI : 10.4000/cybergeo.5532, 2008.

Gumiere, S.J., Le Bissonnais, Y., Raclot, D. and Cheviron, B.: Vegetated filter effects on sedimentological connectivity of agricultural catchments in erosion modelling: a review. Earth Surface Processes and Landforms 36, 3–19, 2011.

Haggett, P. and Chorley, R.J.: Network analysis in geography, Edward Arnold, Science, 348 pp, 1969.

Harvey, A.M.: Coupling between hillslopes and channels in upland fluvial systems: implications for landscape sensitivity, illustrated from the Howgill Fells, northwest England. Catena 42, 225-250, 2001.

Heckmann, T. and Schwanghart, W.: Geomorphic coupling and sediment connectivity in an alpine catchment - exploring sediment cascades using graph theory. Geomorphology 182, 89-103, 2013.

Heckmann, T., Schwanghart, W. and Phillips, J.D.: Graph theory: Recent developments of its application in geomorphology. Geomorphology 243, 130-146, 2015.

Kimberly, A.W., Gardner, R.H. and Turner, M.G.: Landscape connectivity and population distributions in heterogeneous environments. Oikos 78, 151–169, 1997.

Ludwig, J.A., Eager, R.W., Bastin, G.N., Chewings, V.H. and Liedloff, A.C.: A leakiness index for assessing landscape function using remote sensing. Landscape Ecology 17, 157–171, 2002.

McGuinness, J.L., Harrold, L.L. and Edwards, W.M.: Relation of rainfall energy streamflow to sediment yield from small and large watersheds. Journal of Soil and Water Conservation 26, 233-235, 1971.

Newman, M.E.J.: Networks: An Introduction, Oxford University Press, 2010.

Pumain, D. and Saint-Julien T.: Analyse spatiale : les localisations, Cursus, Armand Colin, Paris, 192 pp, 2010.

Renard, K., Foster, G.R., Weessies, G.A., Mc Cool, D.K. and Yodler, D..C. Predicting soil erosion by water: a guide to conservation planning with the Revised Universal Soil Loss Equation (RUSLE). U.S. Department of Agriculture. Agriculture Handbook 703, 1-384, 1997.

Schumm, S., 2005. River variability and complexity, Cambridge University Press, 219 p, 2005.

Tischendorf, L and and Fahrig, L.: How should we measure landscape connectivity? Landscape Ecology 15, 633–641, 2000.

Turnbull, L., Wainwright, J., Brazier, R.E.: A conceptual framework for understanding semi-arid land degradation: ecohydrological interactions across multiple-space and time scales. Ecohydrology 1, 23–34, 2008.

Uezu, A., Metzger, J.P. and Vielliard, J.M.E.: Effects of structural and functional connectivity and patch size on the abundance of seven Atlantic forest bird species. Biological Conservation 123, 507–519, 2005.

Viel V.: Analyse spatiale et temporelle des transferts sédimentaires dans les hydrosystèmes normands. Exemple du bassin versant de la Seulles. Ph-D Thesis, Université de Caen, 382 pp, 2012.

Wainwright, J., Turnbull, L., Ibrahim, T.G., Lexartza-Artza, I., Thornton, S.F. and Brazier, R.E.: Linking environmental regimes, space and time: interpretations of structural and functional connectivity. Geomorphology, 126: 387–404, 2011.

Walker, R.G.: Perspective, facies modelling and sequence stratigraphy. Journal of Sedimentary Petrology 60, 777-786, 1990.

Walling, D.E.: The sediment delivery problem. Hydrology, 69, 209-237, 1983.

Wischmeier, W.H. and Smith, D.D.: Predicting Rainfall Erosion Losses - A Guide to Conservation Planning. U.S. Department of Agriculture. Agriculture Handbook 537, 1-58, 1978.

With, K.A., Gardner, R.H. and Turner, M.G.: Landscape connectivity and population distributions in heterogeneous environments. Oikos 78, 151–169, 1997.

	A	B	C	D	E	F	G
A	1	0	0	1	0	0	0
B	0	1	1	0	0	0	0
C	0	0	1	1	0	0	0
D	0	0	0	1	1	0	0
E	0	0	0	0	1	1	0
F	0	0	0	0	0	1	0
G	0	0	0	0	1	0	1

Table 1: Adjacency matrix of the virtual sediment cascade

	0	**1**	**2**	**3**	**4**	**5**	**F^{i}_{jo}**	**Fi**
A	**1**	**0**	**0**	**0**	**0**	**0**	**1**	**0,05**
B	**1**	**0**	**0**	**0**	**0**	**0**	**1**	**0,05**
C	**1**	**1**	**0**	**0**	**0**	**0**	**2**	**0,09**
D	**1**	**2**	**1**	**0**	**0**	**0**	**4**	**0,18**
E	**1**	**2**	**2**	**1**	**0**	**0**	**6**	**0,27**
F	**1**	**1**	**2**	**2**	**1**	**0**	**7**	**0,32**
G	**1**	**0**	**0**	**0**	**0**	**0**	**1**	**0,05**
						Total	**22**	

Table 2: Analysis of the potential sediment flow within the sediment cascade. The first rows correspond to the iterations simulating the evacuation of sediments. At the right, the rows detail the calculation of the Flow index.

Earth Surf. Dynam. Discuss., doi:10.5194/esurf-2016-55, 2016
Manuscript under review for journal Earth Surf. Dynam.
Published: 8 November 2016

	A	B	C	D	E	F	G	$D_{i,}$	Ai
A	**0**	**0**	**0**	**1**	**2**	**3**	**0**	**6**	**0,17**
B	**0**	**0**	**1**	**3**	**4**	**5**	**0**	**13**	**0,37**
C	**0**	**0**	**0**	**2**	**3**	**4**	**0**	**9**	**0,29**
D	**0**	**0**	**0**	**0**	**1**	**2**	**0**	**3**	**0,26**
E	**0**	**0**	**0**	**0**	**0**	**1**	**0**	**1**	**0,34**
F	**0**	**0**	**0**	**0**	**0**	**0**	**0**	**0**	**0,49**
G	**0**	**0**	**0**	**0**	**1**	**2**	**0**	**3**	**0,09**
$D_{.i}$	**0**	**0**	**1**	**6**	**11**	**17**	**0**	**35**	

Table 3: Distance matrix (origin-to-destination) of the virtual sediment cascade. At the right, the rows detail the calculation of the accessibility index.

	0	1	2	3	4	5	F^{i}_{jo}	Fi	Ai	ICi
A	**1**	**0**	**0**	**0**	**0**	**0**	**1**	**0,03**	**0,18**	**0,20**
B	**2**	**0**	**0**	**0**	**0**	**0**	**2**	**0,07**	**0,35**	**0,20**
C	**1**	**2**	**0**	**0**	**0**	**0**	**3**	**0,10**	**0,28**	**0,38**
D	**1**	**2**	**3**	**0**	**0**	**0**	**6**	**0,21**	**0,25**	**0,83**
E	**1**	**2**	**2**	**3**	**0**	**0**	**8**	**0,28**	**0,33**	**0,85**
F	**1**	**1**	**2**	**2**	**3**	**0**	**9**	**0,31**	**0,55**	**0,56**
G	**0**	**0**	**0**	**0**	**0**	**0**	**0**	**0,00**	**0,08**	**0,00**
						Total	**29**			

Table 4: Analysis of the potential flow and calculation of connectivity following a new parameterization. The rows indicate the patterns of sediment evacuatuation at each iteration of the simulation. Source B provides twice more sediments and the distance between E and F is twice than during the initial conditions.

Earth Surf. Dynam. Discuss., doi:10.5194/esurf-2016-55, 2016
Manuscript under review for journal Earth Surf. Dynam.
Published: 8 November 2016

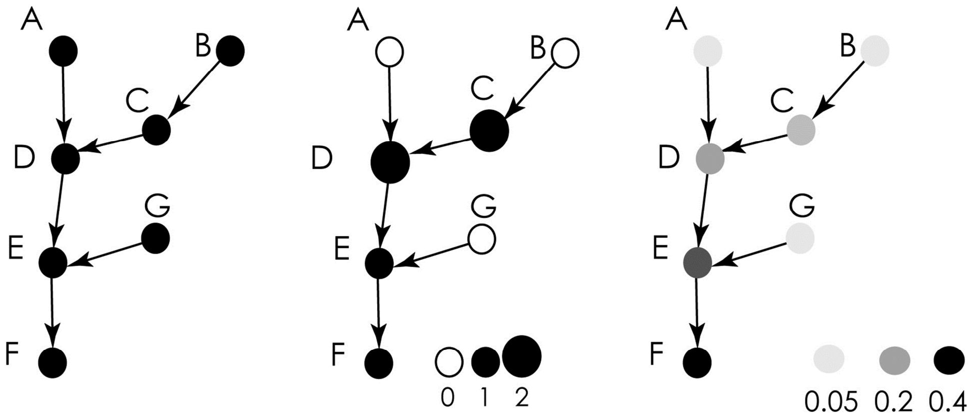

Figure 1: The virtual sediment cascade. A: The structure of the cascade, represented by a graph. B: Potential flow of sediments after one iteration during the simulation. C: Map of flow index values.

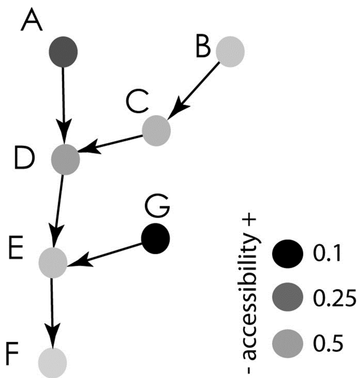

Figure 2: Assessment of accessibility index within the virtual sediment cascade.

Earth Surf. Dynam. Discuss., doi:10.5194/esurf-2016-55, 2016
Manuscript under review for journal Earth Surf. Dynam.
Published: 8 November 2016

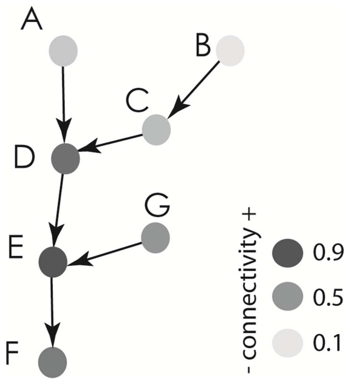

Figure 3: Assessment of connectivity index within the virtual sediment cascade.

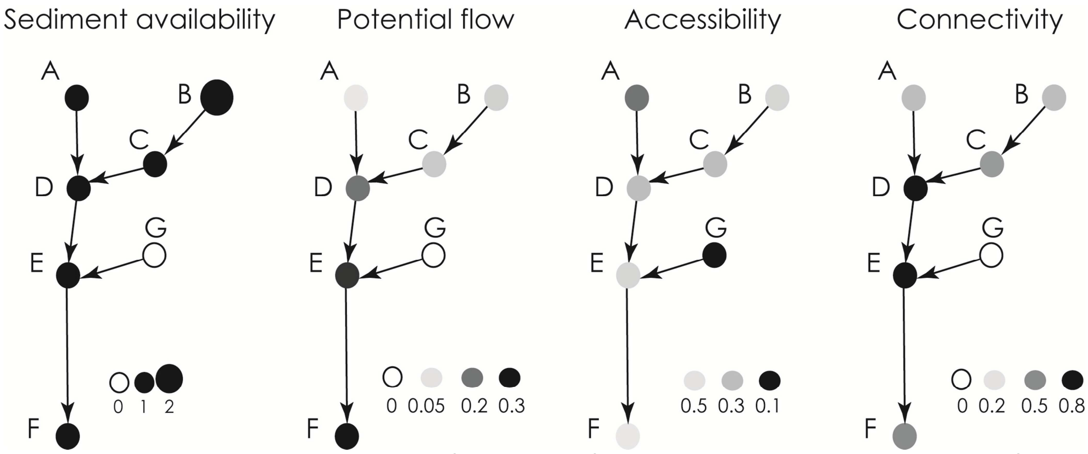

Figure 4: Flow, accessibility and connectivity indices following a modified parameterization. Note how the connectivity of node D is reinforced, and connectivity of F gets lower.

Earth Surf. Dynam. Discuss., doi:10.5194/esurf-2016-55, 2016
Manuscript under review for journal Earth Surf. Dynam.
Published: 8 November 2016

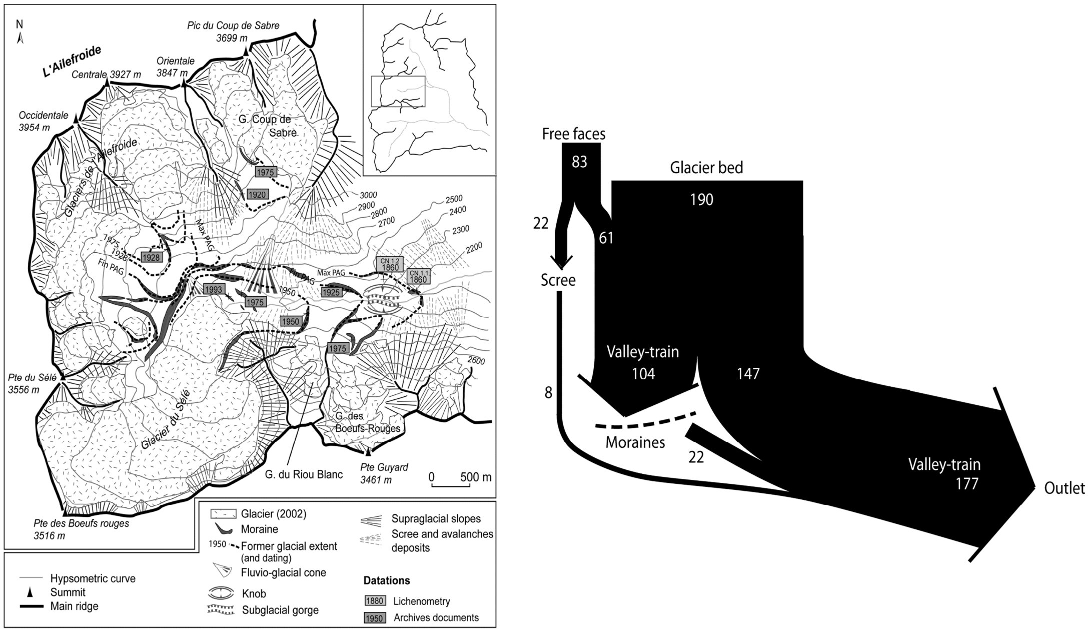

Figure 5: Celse-Nière catchment and sediment cascade. A: Geomorphological map of the study area. Note the various morainic ridges that disconnect the sediment cascade. B: Synthetic pattern of the potential flow within the sediment cascade.

Earth Surf. Dynam. Discuss., doi:10.5194/esurf-2016-55, 2016
Manuscript under review for journal Earth Surf. Dynam.
Published: 8 November 2016

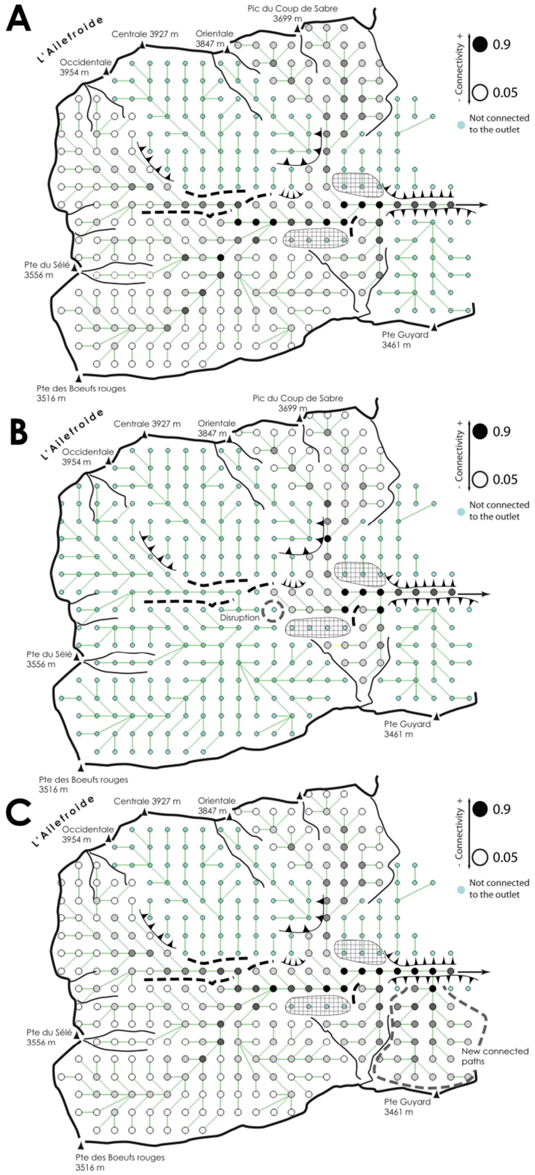

Figure 6: Assessment of connectivity. A: Current structure of the cascade. B: Connectivity map after the simulation of a disruption at Sélé toe. C: Connectivity map after the simulation of a reconnection at Guyard outlet.